Testing the Hypothesis That Charge Exchange Can Cause a Two-Phase Decay

M.W. Liemohn and J.U. Kozyra

Atmospheric, Oceanic, and Space Sciences Department, University of Michigan, Ann Arbor

We test the hypothesis that a two-phase decay of the ring current energy content can be produced by the differential charge exchange loss rates of hot O^+ and hot H^+. Results are presented from idealized simulations of ring current decay and show that, for realistic plasma boundary conditions, a two-phase decay can only be created by the transition from flow-out to charge exchange dominance of ring current loss. Differential charge exchange between hot ($E > 40$ keV) O^+ and hot H^+ cannot produce the observed two-phase decay signature for several reasons. First, there are always significant levels of low-energy ($E < 10$ keV) H^+ present in the injected plasma, which charge exchanges rapidly and makes the H^+ loss rate comparable to or greater than the O^+ loss rate. Second, the ring current is spread over a wide range of *L* values, and the total charge exchange loss rate is an integral value that does not suddenly change. Third, this integral loss rate is too slow (at least in the results presented here) to create a rapid loss of ring current energy content. Other possible causes of two-phase decay signatures in the storm-time *Dst* index are briefly discussed.

1. INTRODUCTION

For many years, it was commonly believed that the main phase of a magnetic storm rapidly produced a symmetric ring current that provided a majority fraction of the *Dst* index decrease [e.g., *Lyons and Williams*, 1980; *Lee et al*., 1983]. More specifically, the ring current is the dominant contributor to the *Dst** index, which is *Dst* with the influences from the magnetopause current, quiet time offset, and induced Earth currents removed. Loss of the trapped ring current energy (and thus recovery of the *Dst** index toward zero) was believed to occur dominantly through charge exchange with the neutral hydrogen geocorona, with minor contributions from Coulomb drag energy loss and scattering of particles into the loss cone by wave-particle interactions [see the review by *Daglis et al*., 1999]. In fact, the two-phase decay of large magnetic storms was believed to be the result of the large differences between the charge exchange lifetimes of oxygen and hydrogen ions with energies above 50 keV [*Tinsley and Akasofu*, 1982; *Hamilton et al*., 1988]. The much more rapid removal of oxygen ions was thought to be the cause of the fast loss lifetimes during the early recovery phase. By the end of the early recovery phase, the ring current was significantly depleted in oxygen relative to protons. The long charge-exchange lifetimes of the proton component dominated the late recovery phase. The preferential removal of oxygen ions by charge exchange with the hydrogen geocorona in the early recovery phase was thought to drive the observed dramatic composition changes that are correlated closely with the ring current recovery [*Hamilton et al*., 1988; *Daglis,* 1997].

It is now understood, however, that the partial ring current far exceeds the symmetric ring current throughout the entire main phase of magnetic storms (which typically last from several hours to more than a day) and into the early recovery phase. This has been shown both theoretically [e.g., *Takahashi et al*., 1990, 1991; *Ebihara and Ejiri*, 1998, 2000;

Magnetosphere Modeling
Geophysical Monograph Series XXX

10.1029/XXXGMXX

Jordanova et al., 1998; *Liemohn et al*., 1999, 2001a, b; *Kozyra et al*., 2002] as well as observationally [e.g., *Greenspan and Hamilton*, 2000; *Jorgensen et al.*, 2001; *Pollock et al*., 2001; *Mitchell et al*., 2001; *Reeves and Spence*, 2001; *Soraas et al*., 2002, 2003]. A major symmetric ring current component only appears in the late recovery phase. The partial ring current is formed as energetic ions in the inner plasma sheet are convected deep into the dipolar regions under the action of an enhanced convection electric field. These particles move on open drift paths that intersect the dayside magnetopause and thus rapid particle loss occurs through this boundary [*Liemohn et al*., 1999]. Of course, the removal of ions from these open drift paths by charge exchange interactions and precipitation (which results from nonadiabatic scattering of the ions moving along highly stretched magnetic field lines) decreases the ring current lifetime even further; but these are secondary effects [c.f., *Kozyra et al*., 1998, 2002; *Liemohn et al*., 1999]. As the early recovery phase of the storm begins, the convection electric field weakens. This decrease drives the conversion of open to closed drift paths; in other words, the conversion from a partial to a symmetric ring current. Time scales in the late recovery phase are dominated by charge exchange losses of high-energy protons and thus are long compared to those in the early recovery phase.

The changeover from rapid removal at the dayside magnetopause during the main and early recovery phases to much-slower charge-exchange removal of trapped ring current particles during the late recovery phase accounts for the two distinctly different lifetimes that dominate the ring current recovery [*Jordanova et al*., 2003; *Kozyra and Liemohn*, 2003]. That is, continued convection into the recovery phase causes the initial fast recovery of the ring current, and a rapid shut-off of this flowout suddenly stops this loss process, allowing the slower loss processes to dominate the recovery time scale. The timing of the convection decrease relative to the plasma sheet density decrease is critical. The density reduction must happen first for a rapid decay phase to occur. During a period of high convection and low source population intensity, the high-density plasma injected during the main phase is quickly flushed from the inner magnetosphere, being replaced by less-dense plasma.

The debate remains alive, however. For instance, *Feldstein et al*. [2000] and *Ohtani et al*. [2001] argue that a rapid shut off the tail current can cause a significant recovery of the *Dst* index. *Walt and Voss* [2001] found that particle precipitation causes fast loss lifetimes that might be responsible for the two-phase decay of the ring current. *O'Brien et al*. [2002] statistically analyzed the recovery rate of *Dst* for storms with rapid shut-off of the convection strength versus those with gradual shut-off (continued convection). They found that the two groups of storms had statistically identical decay rates. *Daglis et al*. [2003] argued that differential charge exchange loss between hot O^+ and H^+ is a major factor in the two-phase decay recovery for some storms.

This study addresses the relationship between charge exchange losses and flowout out losses. A series of numerical experiments are conducted with idealized input conditions to parametrically examine the relative importance of flowout and charge exchange to the decay rate of the ring current total energy content. In particular, the study will assess the validity of the hypothesis that the differential charge exchange rates between energetic O^+ and H^+ is sufficient to produce a two-phase decay. The other possibilities for two-phase decay production mentioned above will be discussed but not quantitatively investigated. In addition, a list of caveats to the interpretation and application of these results is given.

2. NUMERICAL APPROACH

This study uses results from the Michigan version of the ring current-atmosphere interaction model (RAM), a kinetic transport code that solves the gyration and bounce-averaged Boltzmann equation inside of geosynchronous orbit. *Fok et al*. [1993] was the first to publish results from this model, and she continues to maintain a version of this code [e.g., *Fok et al*., 2003]. The code remained at Michigan as well, and the next development series began with *Jordanova et al*. [1996], who also continues to use the code [e.g., *Jordanova et al*., 2003]. The version used for the present study is described by *Liemohn et al*. [2001a, 2004]. It uses second-order accurate numerical schemes to determine the hot ion phase-space distribution in the inner magnetosphere as a function of time, equatorial plane location, energy, and equatorial pitch angle. Sources are specified by geosynchronous orbit plasma data across the nightside outer boundary. Loss mechanisms include the flow of plasma out the dayside outer boundary, precipitation of particles into the upper atmosphere, pitch angle scattering and drag from Coulomb collisions with the plasmasphere (using the *Ober et al*. [1997] thermal plasma code), and charge exchange with the neutral hydrogen geocorona (using the *Rairden et al*. [1986] geocoronal model). A dipole magnetic field is assumed. The magnetopause is not explicitly defined in these simulations. Therefore, flow-out losses are losses through the dayside outer boundary, which is at geosynchronous altitude.

For the present study, idealized inputs were specified for each simulation. The electric field description chosen for these experiments is the Volland-Stern two-cell convection model [*Volland*, 1973; *Stern*, 1975], with nominal shielding ($\gamma = 2$) and the Kp-dependent activity parameter defined by *Maynard and Chen* [1975]. While this is a very simplistic field model, it has been used effectively to reproduce

the inner magnetospheric plasma dynamics with reasonable accuracy [e.g. *Jordanova et al*., 1998, 2003; *Kozyra et al*., 1998; *Ebihara and Ejiri*, 1998, 2000]. Furthermore, statistical analyses of inner magnetospheric plasma observations have found that the shielded Volland-Stern electric field is very good at reproducing the observations [*Korth et al*., 1999; *Friedel et al*., 2001]. In the simulations conducted for this study, artificial "Kp" time series were created for each numerical experiment, with step-function changes in the activity level separating intervals of constant convection strength.

The second half of the idealized input specification is the nightside outer boundary condition for the hot ions. A kappa distribution (with $\kappa = 5$) is assumed with identical characteristics at all local times. The near-Earth plasma sheet characteristic energy (E_{PS}) is held constant throughout the simulation (7 keV unless specified), while the density (N_{PS}) is changed at certain times in each run (again, with step function changes separating intervals of constant density). The chosen values are typical for the near-Earth plasma sheet [*McComas et al*., 1993; *Birn et al*., 1997; *Borovsky et al*., 1998]. The composition of the boundary condition plasma is specified to be equal densities of H^+ and O^+ (each equal to N_{PS}). Because the hot ion species are not coupled for these simulations (that is, the electric field is specified rather than self-consistently calculated), the run for each species can be conducted separately and the results added later. This also allows for an arbitrary combination of the two species.

In the present study, step-function changes in Kp and N_{PS} are applied. After a 24-hour interval of quiescent values (Kp = 2, $N_{PS} = 0.5$ cm^{-3}), both parameters are increased to disturbed-condition values (Kp = 6.5 or 9, $N_{PS} = 4$ cm^{-3}). These high values are held constant for 12 hours of run time to reach a quasi-steady-state level in the inner magnetosphere. This is the initial condition for all of the numerical experiments shown below. The down-step for Kp and N_{PS} is then applied at either the 1-hour or the 4-hour mark (sometimes together, other times staggered), dropping the parameters back to their quiescent levels.

The chosen boundary and input conditions are not particularly realistic. For instance, ion distributions are not identical across the nightside, the magnetic field is not dipolar, factor of 8 step-function changes in density and convection are rare, and the inner magnetospheric electric field is modulated by the hot ion pressures in this region. The simulation results are thought to be useful, though, because they demonstrate the relative dominance of flow-out versus charge-exchange losses in modulating the recovery of the ring current. More on these caveats to the study results are given below in the Discussion.

Kp is a quasi-logarithmic index, and so a more useful quantity to discuss is the westward convection electric field at midnight at the outer simulation boundary. Figure 1 shows

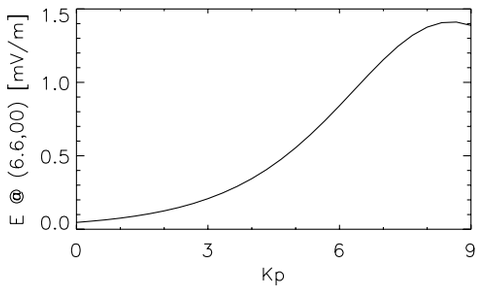

Figure 1. Electric field strength at $R = 6.6$ R_E at magnetic local midnight with respect to Kp for the shielded Volland-Stern electric potential description with the Maynard-Chen activity dependence.

the relationship between this electric field value and Kp for a shielded Volland-Stern description. For Kp = 2, the electric field is 0.125 mV/m. For Kp = 6.5, the electric field is 1.0 mV/m. This Kp step produces a factor of 8 increase in the convection strength, matching the factor of 8 increases applied to N_{PS}. Two cases use Kp = 9, which yields an electric field of 1.4 mV/m. This is more than 11 times bigger than the Kp = 2 electric field, and represents extreme geomagnetic activity.

3. RESULTS

The purpose of this study is to examine the ability of flowout loss and charge exchange loss to produce a two-phase decay. While there are many other loss mechanisms acting on the storm-time ring current, these two are the largest [e.g., *Liemohn et al*., 1999; *Kozyra et al*., 2002] and they are the center of the controversy around the two-phase-decay phenomenon [e.g., *Daglis and Kozyra*, 2002; *Daglis et al*., 2003].

3.1. Down-Step Experiments

Figure 2 shows results from a simulation in which N_{PS} drops 3 hours before Kp. Figures 2a and 2b show the time series of N_{PS} and the midnight outer boundary electric field, respectively. This is an example of continued convection, but with decreased plasma sheet density, during the recovery phase of a magnetic storm.

The total energy of the hot ion population inside of geosynchronous orbit E_{RC} is shown in Figure 2c, along with the totals for H^+ and O^+ separately. The solid curve in Figure 2c has the appearance of a two-phase decay. It begins at 10.1 PJ, decreasing to 4.93 PJ by $t = 4$ h, and eventually dropping to 3.24 PJ by $t = 12$ h. There is a definite kink in the E_{RC} curve at $t = 4$ h, with the loss rate becoming much smaller after the down-step of the electric field. The two species have very

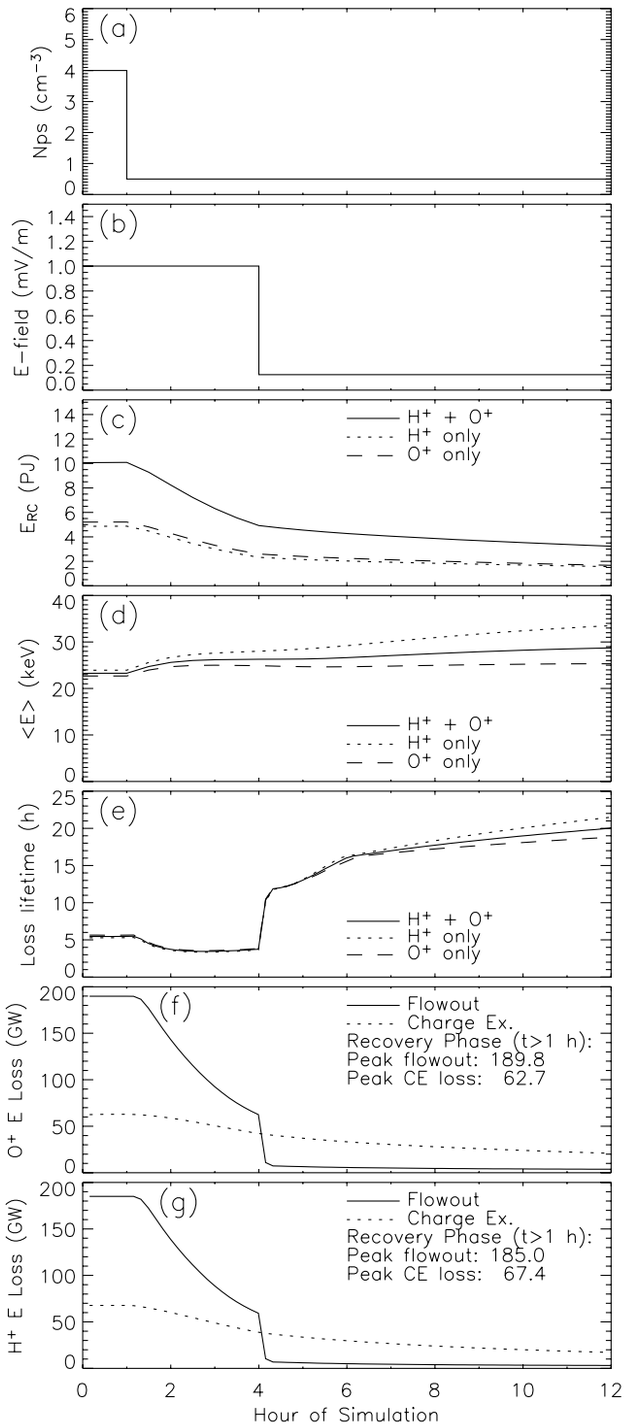

Figure 2. Simulation inputs and results from a numerical experiment in which the plasma sheet density decreases before the convection strength. Shown are the following: (a) plasma density applied at the outer simulation boundary (the same for both H^+ and O^+); (b) the midnight outer boundary electric field strength; (c) the total energy content in the ring current; (d) the average energy of a ring current ion; (e) the pure-loss lifetime for the total energy content; (f) the particle loss rate for O^+ from flowout and charge exchange; and (g) the particle loss rate for H^+ from flowout and charge exchange.

similar total energy values throughout the simulation, with the O^+ curve beginning 0.3 PJ higher than the H^+ value and ending 0.1 PJ higher than H^+ at $t = 12$ h.

Figure 2d presents the average particle energy during the simulation (total amount of energy divided by total number of particles). This is an interesting quantity because both loss processes are dependent on it. Flowout is affected because the drift paths through the inner magnetosphere are influenced by the gradient-curvature drift, which is directly proportional to energy. Charge exchange has energy dependence in both the cross section and the number of targets ($v\Delta t$, the flight distance per time increment). The average energy (H^+ and O^+ together) begins at a steady 23 keV, and then slowly increases to 29 keV by $t = 12$ h. The average energy for H^+ is slightly higher than that for O^+ throughout the simulation.

Liemohn and Kozyra [2003] discussed the calculation of loss lifetimes from ring current simulations. A "pure-loss" time scale can be calculated by dividing the total energy content by the energy loss rate from all processes. For example, at the end of the simulation ($t = 12$ h), the total energy content of the hot ions is 3.24 PJ (1.57 PJ carried by H^+ and 1.67 PJ carried by O^+). The total loss rate from the system at this time is 45.2 GW (20.4 GW departing from the H^+ content and 24.9 GW from O^+). Dividing the latter into the former yields a pure-loss lifetime of 20.0 hours (for H^+ and O^+, the pure-loss lifetimes are 21.5 hours and 18.8 hours, respectively). The "pure-loss" qualifier is added because this loss lifetime is only observed if there is no energy input to the ring current, which is not the case, even during quiet times. Nevertheless, it is useful quantity because it tells about the relative magnitude of the energy loss (compared to the total energy).

Figure 2e shows this pure-loss lifetime from the simulation results. At $t = 0$ h, the loss lifetime is ~5.5 hours. It then decreases to a minimum value of ~4 hours at $t = 3$ h. At $t = 4$ h, there is a sudden jump in the loss lifetime up to ~12 hours, and the lifetime slowly increases to 20 hours by $t = 12$ h. In this latter part of the simulation, the O^+ and H^+ lifetimes split apart a little, with H^+ ending with a loss lifetime of 21.5 hours and O^+ at 19 hours. That is, the total energy of O^+ is being lost slightly faster than that of H^+ (relative to the total energy for each species). This is reflected in the convergence of the dashed and dotted lines in Figure 2c.

The magnitudes of the hot ion losses for O^+ and for H^+ are shown in Figures 2f and 2g, respectively. Only the two

dominant loss processes of dayside flowout and charge exchange are plotted. The peak values during the recovery phase ($t > 1$ h) are listed for each process in each figure. It is seen that flowout energy loss is 3 to 4 times larger than charge exchange at the beginning of the recovery phase (just after $t = 1$ h), and remains larger than charge exchange through the early recovery period (until $t = 4$ h). Once the convection electric field is reduced (at $t = 4$ h), flowout drops to less than 10 GW for each of the species, a level below that for charge exchange at this time (~40 GW). The losses from charge exchange do not show such a dramatic change. Instead, they gradually decrease throughout the recovery phase. While both charge exchange loss rates (H^+ and O^+) end near 20 GW (at $t = 12$ h), they begin at slightly different values, with O^+ starting at 60 GW and H^+ starting at 70 GW.

Note that the energy loss rates are significantly different from the particle loss rates. Because flowout occurs at the outer simulation boundary while charge exchange occurs deep within the simulation domain, the average energies of the particles lost by these two processes are quite different. Therefore, the ratio of flowout-to-charge exchange particle losses is ~8 at $t = 1$ h, dropping to ~4 just before $t = 4$ h, and the two particle loss rates are roughly equal throughout the late recovery phase. The energy loss rate is more applicable to this study, and therefore it is shown in Figure 2.

Figure 3 presents a similar sequence of plots for the opposite ramp-down case, in which the convection electric field is reduced 3 hours prior to the plasma sheet density (see figures 3a and 3b). The resulting total energy content carried by the hot ions in the inner magnetosphere is shown in Figure 3c. There is no visible kink in the curves at $t = 4$ h, or in fact anywhere past $t = 1$ h. The average energy is shown in Figure 3d, again showing that O^+ is slightly cooler than H^+ and that the two are diverging slowly throughout the recovery phase. The pure-loss lifetimes are given in Figure 3e. There is a step-function change from 5 to 15 hours at the time when the electric field is reduced ($t = 1$ h). After this, the loss lifetime slowly increases above 20 hours by the end of the simulation. The magnitudes of the loss rates are shown in the final two panels (Figures 3f and 3g), again showing that the flowout loss rate is much bigger than charge exchange during high convection ($t < 1$ h) but drops below the charge exchange loss rate when the convection strength is reduced ($t > 1$ h). The late recovery phase ($t > 4$ h) flowout energy loss rates for both species are larger for this simulation than for the simulation results presented in Figure 2. This is because of the much lower energy loss rate during the first three hours of the recovery. Therefore, flowout loss is roughly a factor of 2 to 3 less than charge exchange throughout the recovery phase. As in Figure 2, the charge exchange loss rates decrease slowly throughout the simulation, with no sudden changes in the loss rate for either species.

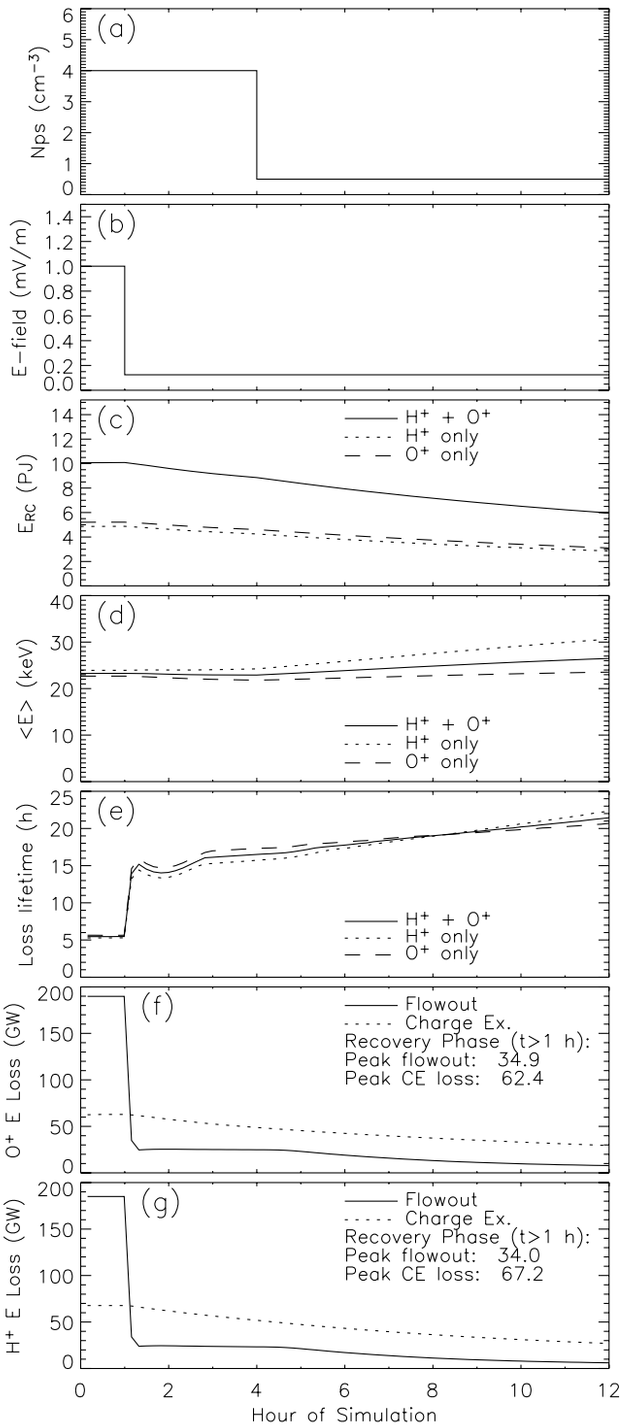

Figure 3. Same as Figure 2 except for a numerical experiment in which the convection strength decreases before the plasma sheet density.

Figure 4 presents a third case in which the electric field and N_{PS} are both reduced simultaneously (Figures 4a and 4b). There is no kink evident in the total energy content of the hot ions for this simulation (Figure 4c), and the ion average energies slowly increase at different rates for the two species (Figure 4d). As in the previously discussed simulation, the loss lifetime shows a sudden increase at $t = 1$ h followed by a slow increase for the rest of the simulation (Figure 4e). The sudden increase in the loss lifetime corresponds to the sharp drop in flowout loss (Figures 4f and 4g), and the subsequent slow rise in the loss lifetime is caused by the slow decrease in the loss rates for both flowout and charge exchange during the rest of the simulation.

3.2. High-Convection Experiments

The results presented thus far are for simulations with Kp ramping down from 6.5 to 2. While Kp = 6.5 is a storm-time value, this isn't the highest value for the index. Stronger convection allows for deeper injection of the plasma sheet ions into the inner magnetosphere. Because the hydrogen geocoronal density increases closer to the Earth, the charge exchange losses should be bigger. Furthermore, the adiabatic acceleration of the particles as they convect radially inward should create more high-energy ring current particles. It is at the high energies that O^+ is preferentially removed via charge exchange. Thus, a higher magnetospheric convection rate should result in more charge exchange loss of O^+, yielding the best opportunity (of the selected numerical experiments) for a charge-exchange-driven two-phase decay of the ring current.

Figure 5 shows results for a ramp-down from Kp = 9, which corresponds to a midnight outer boundary convection electric field strength of 1.4 mV/m. Both input parameters (electric field and N_{PS}) are reduced simultaneously (Figures 5a and 5b). It is seen that the total energy content of the ring current ions has no visible kink (Figure 5c). While the average energies are higher for this simulation than the previous ones (Figure 5d), the loss lifetimes are still quite close early in the recovery phase and diverge rather slowly throughout the simulation (Figure 5e). The loss rates shown in Figures 5f and 5g are very similar to those presented in Figures 4f and 4g, respectively, with slightly higher magnitudes for the charge exchange losses, as expected.

A final numerical experiment to be discussed is a simulation with the plasma sheet characteristic energy E_{PS} set to 20 keV, instead of 7 keV as in the previous 4 runs. Otherwise, the set up is identical to the previous run, with the high convection set to Kp = 9 and both input parameters decreasing simultaneously. This simulation is the most favorable of all of those presented for creating a charge-exchange-driven two-phase decay. The results are shown in Figure 6. The average particle energy is indeed higher than in any of the other

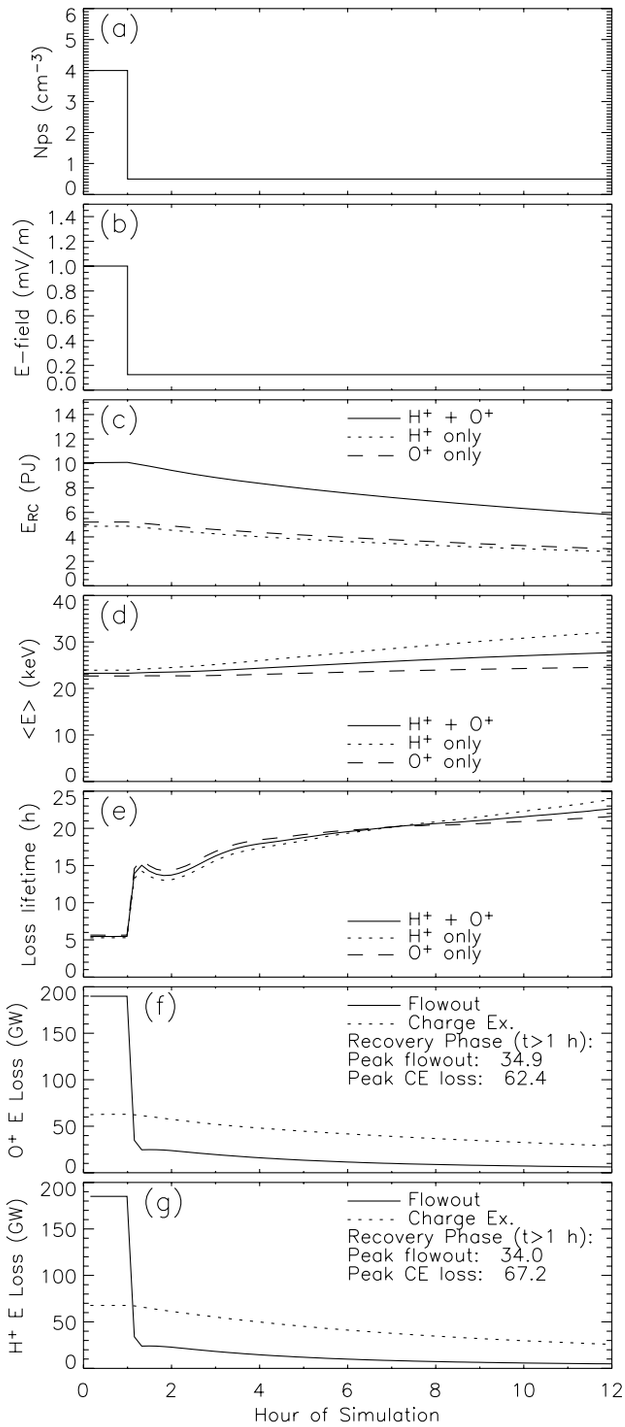

Figure 4. Same as Figure 2 except for a numerical experiment in which the convection strength and plasma sheet density decrease simultaneously.

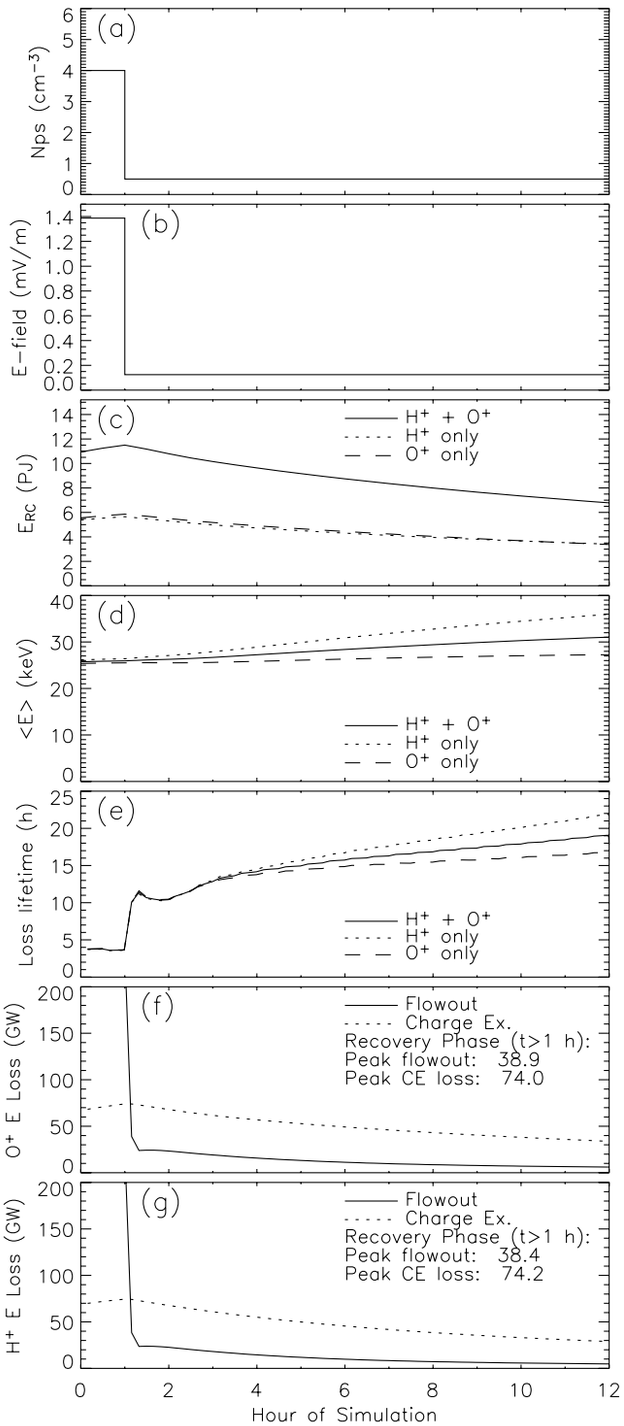

Figure 5. Same as Figure 4 except for a numerical experiment in which the peak convection strength is set to Kp = 9 instead of Kp = 6.5.

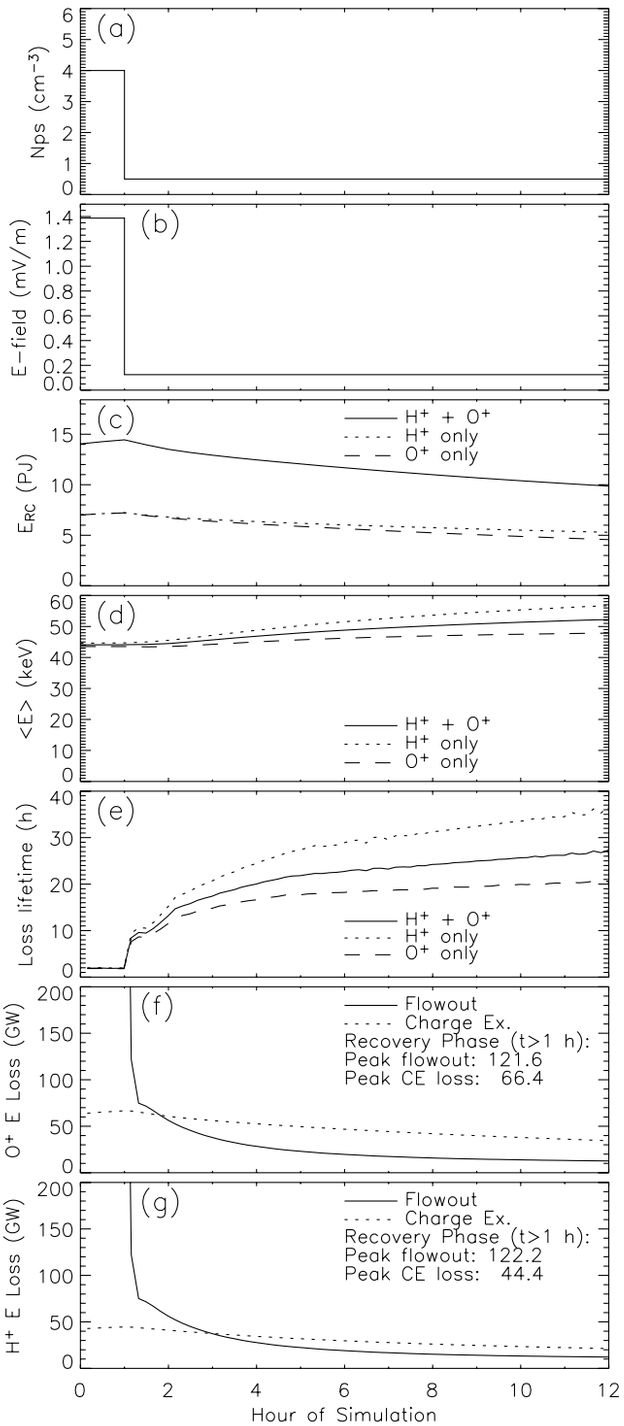

Figure 6. Same as Figure 4 except for a numerical experiment in which the characteristic energy of the plasma sheet is 20 keV instead of 7 keV.

simulations (Figure 6d), but the total energy content still does not show a two-phase decay signature (Figure 6e). In fact, the charge exchange loss rates are less than in the previous run with $E_{PS} = 7$ keV (compare Figures 6f and 6g with 5f and 5g). The peak O^+ charge exchange energy loss rate in Figure 6f is 90% of the peak value in Figure 5f, but the peak H^+ charge exchange rate in Figure 6g is only 65% of the peak value in Figure 5g. So, even though the ratio of the O^+ charge exchange loss rate to that of H^+ is larger for this "hot" simulation (Figure 6) than for the nominal E_{PS} run (Figure 5), the total loss from charge exchange is less, and thus no two-phase decay is produced.

3.3. Composition Experiments

The results thus far have discussed an equal N_{PS} value for H^+ and O^+, resulting in nearly equal energy contents for the two hot ion species. It is useful, however, to assess the compositional dependence of two-phase decay formation. Because the simulations use an imposed electric field description, the results for H^+ and O^+ may be arbitrarily scaled and summed to yield other boundary composition ratios. Figure 7 shows the results of such a calculation, using the results from three of the previously discussed simulations. The plots in the first column (Figures 7a-7d) use the results shown in Figure 4c, in which Kp steps down from 6.5 to 2 simultaneously with the N_{PS} drop. The plots in the second column (Figures 7e-7h) use the results from Figure 5c, where Kp starts at 9 and drops to 2. The plots in the third column (Figures 7i-7l) use the results from Figure 6c, which not only has a Kp drop from 9 to 2 but also has a characteristic energy at the outer boundary of 20 keV (instead of 7 keV). The rows are as follows: the top row shows E_{RC} for H^+ plus half of the O^+ energy content; the second row shows E_{RC} for H^+ plus a tenth of the O^+ energy content; the third row shows E_{RC} for O^+ added to half of the H^+ energy content; and the last row shows E_{RC} for O^+ and a tenth of the H^+ energy content.

It is seen in Figure 7 that none of these compositional combinations for these simulations produce a visible two-phase decay signature in the total energy content of the hot

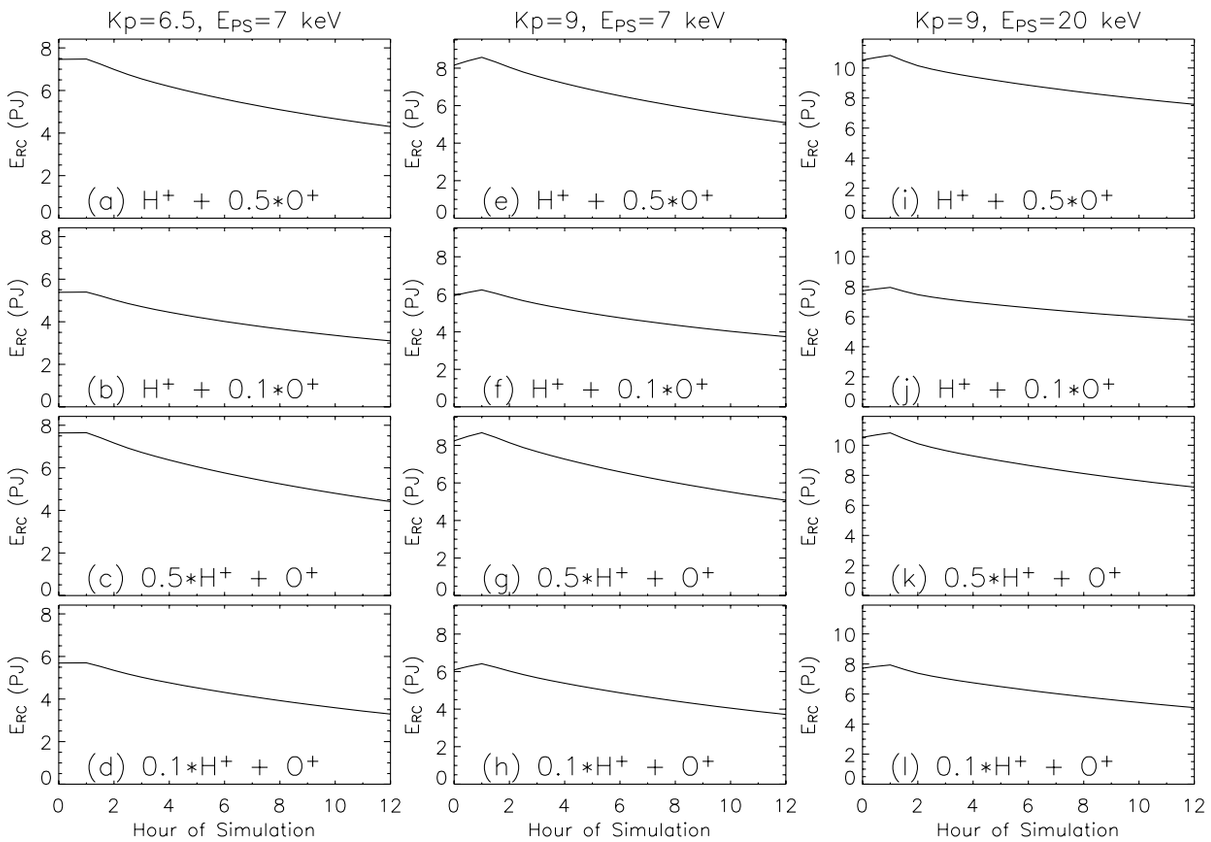

Figure 7. Total energy content for three of the numerical experiments (the 3 columns) with various combinations of the H^+ and O^+ contributions, as marked in each panel.

ions. While the slope of E_{RC} changes throughout the recovery phase in each panel of Figure 7, there is never a sharp transition from a fast to a slow loss rate. It is always a gradual conversion from fast loss to slow loss, regardless of either the ring current boundary conditions (temperature or composition) or the storm-time convection intensity.

3.4. Decay Rate Analysis

In order to quantitatively analyze the structure of the ring current total energy content decay, it is useful to consider ratios of E_{RC} at various times during the simulations. Table 1 presents these ratios for the simulation results presented in Figures 2c, 3c, 4c, 5c, and 6c (from the solid lines in each plot), as well as for each panel in Figure 7. The first column is the fraction that E_{RC} dropped in the first 3 hours of the decay phase. The simulation with high convection continuing after the density decrease (Figure 2c) had a ~50% drop in energy content, while the other simulations had drops in the ~15% range. The simulation with high density continuing after the convection strength reduction (Figure 3c) had the highest fraction remaining, followed by the simulation with the abnormally hot plasma sheet (Figure 6c). The ratios from Figure 7a-7d show that the fraction remaining after 3 hours is smaller when there is relatively more H^+ than O^+, while the fraction is larger when there is relatively more O^+. The next set of numbers (from Figures 7e-7h) show a similar trend, but the fractions are much closer to each other. The third set (from Figures 7i-7l) has the opposite trend, with a higher O^+ relative content producing a lower fraction.

The next two columns of Table 1 show the ratios of E_{RC} after 6 and 9 hours of recovery, respectively, to the peak E_{RC} value just before the recovery began (at $t = 1$ h). The ratios from Figure 2c are well below those from the other simulations. The other simulations continue in their relatively slow decay from the peak E_{RC} value, with the ratios from Figure 6c being the highest in both columns. This is because the high-density source has now turned off for the simulation shown in Figure 3c, and the lower average energy (compare Figures 3e and 6e) leads to a faster recovery rate. The fractions for the plots in Figure 7 continue the trends seen in the first column of numbers.

The final two columns in Table 1 present E_{RC} ratios for 3-to-6 hours into the recovery and 6-to-9 hours into the recovery, respectively. All of these values are quite similar, ranging between 0.82 and 0.93. This shows that all of the simulation results are decreasing at roughly the same pace from $t = 4$ h through $t = 10$ h. Both input parameters are at their quiescent values during this period (in all of the simulations), so any differences in the ratios are primarily caused by different charge exchange loss rates. The slight increase in the values between the fourth and fifth columns in Table 1 is because the particles with faster charge exchange lifetimes are being preferentially removed, leaving only the longer lifetime particles. The fact that the increases in these ratios are slight (1-5%) indicates that the ring current is undergoing a rather slow conversion from fast lifetime dominance to slow lifetime dominance in the decay rate.

4. DISCUSSION

The results presented in Figures 2-7 imply that a two-phase decay is caused by a decrease in the plasma sheet density

Table 1. Ring Current Total Energy Content Ratios.

	($t = 4$ h)/($t = 1$ h)	($t = 7$ h)/($t = 1$ h)	($t = 10$ h)/($t = 1$ h)	($t = 7$ h)/($t = 4$ h)	($t = 10$ h)/($t = 7$ h)
Figure 2c	0.488	0.402	0.350	0.823	0.870
Figure 3c	0.878	0.747	0.646	0.851	0.864
Figure 4c	0.830	0.716	0.626	0.862	0.875
Figure 5c	0.838	0.726	0.639	0.867	0.879
Figure 6c	0.863	0.784	0.720	0.909	0.918
Figure 7a	0.828	0.713	0.625	0.862	0.876
Figure 7b	0.825	0.710	0.623	0.861	0.877
Figure 7c	0.832	0.718	0.628	0.863	0.874
Figure 7d	0.835	0.721	0.630	0.864	0.873
Figure 7e	0.837	0.728	0.642	0.869	0.882
Figure 7f	0.837	0.729	0.646	0.871	0.886
Figure 7g	0.838	0.725	0.636	0.866	0.876
Figure 7h	0.838	0.724	0.631	0.864	0.872
Figure 7i	0.868	0.794	0.734	0.915	0.924
Figure 7j	0.876	0.809	0.754	0.923	0.933
Figure 7k	0.858	0.774	0.706	0.903	0.911
Figure 7l	0.850	0.760	0.685	0.894	0.902

associated with a continued large electric field, followed by a subsequent decrease in the electric field. The decrease in N_{PS} starts the early recovery phase, while the decrease in electric field starts the late recovery phase. The corollary of this conclusion is that charge exchange is incapable of producing a two-phase decay.

4.1. Charge Exchange

The hypothesis was that the charge exchange loss rates for H^+ and O^+ were sufficiently different above ~40 keV to cause a two-phase decay signature. In other words, the transition between the initial rapid loss of hot O^+ and the much slower loss of hot H^+ would create a kink in the total energy content of the ring current. In the kinetic transport model, the influence of charge exchange on the distribution function f is included via an attenuation factor [*Jordanova et al*., 1996],

$$f_{t+dt} = f_t \exp\left(-v\Delta t \sigma_{CE} \left\langle n_H \right\rangle\right) \tag{1}$$

where v is the hot ion velocity, Δt is the time step of the simulation, σ_{CE} is the charge exchange cross section, and $\langle n_H \rangle$ is the bounce-averaged neutral hydrogen density. Equation (1) can be rewritten with a loss lifetime parameter τ_{CE},

$$f_{t+dt} = f_t \exp\left(-\frac{\Delta t}{\tau_{CE}}\right) \tag{2}$$

where

$$\tau_{CE} = \frac{1}{v\sigma_{CE}\left\langle n_H \right\rangle} \tag{3}$$

is a function of hot ion energy, equatorial pitch angle, radial distance, and hot ion species. Figure 8 presents a few curves of τ_{CE} (in hours) versus hot ion energy (in keV) for H^+ and O^+ at several L values. All of these results are for an equatorial pitch angle of 45°. Figure 8 shows that τ_{CE} can vary over several orders of magnitude as these parameters are changed. Most notably, τ_{CE} for H^+ is always lower than τ_{CE} for O^+ at energies below 40 keV. At $L = 6.5$, this crossover value is above 100 hours (more than 4 days). For $L = 4.5$, the crossover value is ~40 hours, and for $L = 2.5$, H^+ and O^+ have equal τ_{CE} values at ~9 hours. The H^+ loss lifetime quickly rises above 40 keV, but the O^+ loss lifetime is relatively flat at these higher energies. Thus, there is a large disparity in the loss lifetime at high energies, and the hot O^+ ions should be preferentially removed long before the hot H^+ ions are depleted.

The problem is the magnitude of the loss lifetime. The entire ring current must reside at $L = 2.5$ in order to get a charge

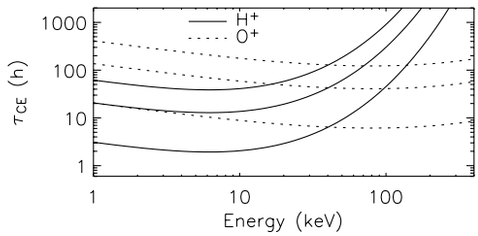

Figure 8. Charge exchange loss lifetimes versus hot ion energy as a function of radial distance and species. The solid curves show the values for H^+ and the dotted curves show the values for O^+. For each species, there are 3 curves. The highest curve is for $L = 6.5$, the middle curve is for $L = 4.5$, and the lowest curve is for $L = 2.5$. All results are for a hot ion equatorial pitch angle of 45°.

exchange loss lifetime for the total energy content below 10 hours. Moving the ring current just one Earth radius (R_E) outward doubles the O^+ τ_{CE} value (from 10 to 20 hours), and moving it out another R_E doubles the O^+ τ_{CE} again (up to 40 hours). It was shown in Figures 5 and 6 that, even with the application of the largest possible convection strength from the *Maynard and Chen* [1975] activity relationship for the shielded Volland-Stern field, charge exchange can only yield a 10-15 hour loss lifetime for the early recovery phase of the ring current. Conversely, flowout loss is capable of producing a 4-hour loss lifetime with only a moderately high Kp value (see Figure 2).

Compare this with the *O'Brien et al*. [2002] study. They concluded that the recovery of *Dst* is statistically identical for storms with or without continued high convection. This conclusion is compatible with the conclusion of the present study. The important difference is that the plasma sheet density must be dramatically reduced prior to the reduction in convection. If the density reduction is only slight, then there will be significant injection of new plasma into the inner magnetosphere. The rapid removal of the high-density partial ring current must be accompanied by a very weak injection from the tail in order to produce a two-phase decay. When the two input parameters are decreased simultaneously, a two-phase decay is not produced.

Another issue is the relative magnitudes of the H^+ and O^+ charge exchange loss rates. The expectation was that O^+ would have a larger loss rate because of the short loss lifetimes at high energies. This was not observed in the results presented in the previous section. The reason for this is that H^+ is rapidly removed via charge exchange at energies below 40 keV. In the 5-10 keV energy range, the loss lifetime for H^+ at $L = 6.5$ is ~25 hours and at $L = 2.5$ it is less than 2 hours. The O^+ τ_{CE} values are nearly an order of magnitude larger at these energies. The relatively fast removal of H^+ in the low-energy range significantly contributes to the total loss rate. In fact, it accounts for a majority of the H^+ charge exchange

loss rate. Because there are more particles in the low-energy range than the high-energy range, H^+ has a higher charge exchange loss rate than O^+ in all of the simulation results presented in this study.

4.2. Energy Content Recovery

Table 1 highlights this disparity in the loss rate between flowout and charge exchange. The fastest drop in the total energy content of the ring current occurs during a flowout-dominated period. This fast drop only occurs when convection is strong and the plasma sheet density is low. The fractional decrease in the total energy content is much slower during all of the periods when charge exchange was either comparable to or greater than the flowout loss rate (which only occurs during low convection times).

Figure 7 and Table 1 presented results for E_{RC} recovery as a function of boundary condition composition. All of the plots showed a relatively slow conversion from shorter loss lifetimes to longer loss lifetimes, and therefore did not produce a two-phase decay. The rate of recovery, however, is slightly different for each plot. Figures 7a-7d (and the corresponding fractions in Table 1) showed a trend of more H^+ resulting in faster decay. This is because of the E_{PS} value (7 keV) for this simulation. There is an abundance of low-energy H^+ leaving the system through charge exchange, resulting in a higher energy loss rate for H^+ than for O^+.

Figures 7e-7h had the same trend as Figures 7a-7d, but with loss rates that were much closer together. The fractions of remaining E_{RC} (the first 3 columns in Table 1) are also higher than the fractions from Figures 7a-7d, indicating that the energy loss was slower. Both of these trends are because of the higher convection strength, which has several effects. First, it injects the plasma deeper. The ions undergo more adiabatic energization, resulting in a bigger differential between the H^+ and O^+ charge exchange rates. Secondly, charge exchange is faster because of the higher geocoronal density closer to the Earth. The third influence is that the particles are swept through the inner magnetosphere faster, resulting in less total attenuation of the ions due to charge exchange. All three of these effects produce more O^+ charge exchange loss relative to H^+ charge exchange. The third effect is responsible for the overall decrease in the charge exchange loss rate, resulting in the higher fractions in Table 1.

Figure 7i-7l showed the opposite trend from the previous two sets of results. That is, a higher relative O^+ energy content resulted in a faster recovery. This is because of the unusually high E_{PS} value (20 keV) for this simulation as well as the high convection strength during the main phase. These two effects produce a much higher average energy of the ring current ions than for the other simulations (compare Figure 6d with Figures 4d and 5d). The differential charge exchange loss lifetime between O^+ and H^+ for E > 40 keV results in an O^+-dominated ring current yielding a faster decay rate than an H^+-dominated one.

This brings up the issue of average ion energy in the numerical experiments. Figures 2-6 show <E> from 20 keV to 60 keV. Q1
In general, <E> is 2-3 times higher than E_{PS} during the main phase, and this ratio increases to 3-5 by $t = 12$ h. Note that this is an average over the entire simulation domain, and therefore the large flux tubes in the outer simulation domain can significantly contribute to the average energy. This is true even though the equatorial plane density and pressure are much lower here than at the peak of the ring current (which is typically inside of 4 R_E) [e.g., *Liemohn et al*., 2001a, b]. Because of adiabatic energization, the local average energy is much higher at the peak of the ring current than out near the simulation boundaries.

A logical question to ask is whether there is observational evidence for step-function-like decreases in either convection or plasma sheet density, particularly the case of the density decreasing before the convection. An excellent example of this is the September 25, 1998 storm, which has this pattern of input decreases and also exhibits a clear two-phase *Dst** decay [see *Liemohn et al*., 1999, 2001a]. Whether this is a typical case or a rare occurrence is unknown. However, the authors of the *O'Brien et al*. [2002] study are pursuing a follow-up to their statistical analysis of *Dst* decay [T.P. *O'Brien*, personal communication, 2004]. Specifically, they are investigating the timing of plasma sheet versus convection shut-offs and the resulting *Dst* time series. The result should be an observational test of this hypothesis.

4.3. Comparisons and Caveats

It should be noted that the total ion energy content of the hot ions in the inner magnetosphere can be related to the magnetic perturbation at Earth through the Dessler-Parker-Sckopke (DPS) relation [*Dessler and Parker*, 1959; *Sckopke*, 1966]. For the Earth, this relation is one nT of southward magnetic deflection for every 0.04 PJ of energy content (that is, multiply the energy content numbers by −25 to yield magnetic perturbation in nT). Because this introduces an extra layer of assumptions into the model results, the conversion is not performed here. Furthermore, the energy content results are relative numbers because the magnitude is scalable by the plasma sheet density for each hot ion species. Many studies use the DPS formula, however, with success at reproducing the observed magnetic perturbation [e.g., *Kozyra et al*., 1998, 2002; *Jordanova et al*., 1998, 2003; *Greenspan and Hamilton*, 2000; *Liemohn et al*., 2001a]. Therefore, a two-phase decay in the ring current total energy content most likely produces a two-phase decay in the *Dst* index.

Figures 2-6 showed energy loss rates from the various numerical experiments. It was noted that the particle loss

rates have a different relative relationship between flowout and charge exchange. In general, the energy loss rate is a more relevant quantity because it can be directly related to a change in *Dst* (through the DPS relation). However, the particle loss rate is sometimes important, especially when interpreting energetic neutral atom observations. Therefore, care must be taken to not confuse these two loss rates because they are not directly interchangeable.

Walt and Voss [2001] concluded that wave-particle interactions elevate particle precipitation losses to a level capable of producing a rapid initial recovery of the ring current. Other studies have shown that wave-induced particle precipitation is a minor component of the total loss rate from the ring current [e.g., *Jordanova et al*., 1998, 2001; *Soraas et al*., 2002, 2003; *Khazanov et al*., 2002, 2003b]. In fact, particle precipitation losses on the nightside from the injection process are often larger than the losses from wave-particle interactions [e.g., *Jordanova et al*., 2001; *Soraas et al*., 2002]. The present study does not address wave-particle interactions as a source of two-phase decay, but if precipitation is able cause this phenomenon, it is most likely only under rare and special circumstances.

An alternative explanation for two-phase decay formation is the rapid reduction of the tail current. It has been shown that the tail current contributes up to a 25 nT decrease in the *Dst* index [e.g., *Turner et al*., 2000], which can be a significant (but minor) fraction of the total perturbation during a magnetic storm. A sudden decrease in the tail current can therefore cause a sudden recovery of the *Dst* index [e.g., *Feldstein et al*., 2000; *Ohtani et al*., 2001]. Observationally, these recoveries from abrupt changes in the tail current are on the order of 20 nT [*Friedrich et al*., 1999; *Ohtani et al*., 2001]. During a major storm with the minimum *Dst* at –200 nT or below, this is a minor perturbation to the overall recovery rate. It is significant, however, when examining the rapid fluctuations of the *Dst* index (or its one-minute-resolution counterpart, SYM-H). Furthermore, *Liemohn* [2003] showed that the commonly used DPS relation implicitly includes a truncation current when the plasma pressure just inside the outer boundary of the integration volume is nonzero. This truncation current is a crude approximation of the tail current, but the real issue is that the DPS relation overpredicts the perturbation from the currents inside the integration volume, and that this overprediction varies with time. Therefore, great care must be taken in equating changes in the *Dst* index with changes in the ring current. Specifically for this study, a two-phase decay in the *Dst* index may not be a two-phase decay in the ring current.

It is necessary to explain some caveats to the general applicability of these results. For instance, the initial condition for the presented simulations was essentially a steady-state solution for constant, high convection and high plasma sheet density. This neglects the radial diffusion of the high-energy particles into the inner magnetosphere from electric field fluctuations [e.g., *Chen et al*., 1993, 1994; *Khazanov et al*., 2004a, b]. Inclusion of this process would increase the high-energy portion of the ring current ion distribution in the inner magnetosphere, and would alter the charge exchange loss lifetime (lowering it if O^+ is dominant, raising it if H^+ is dominant). The application of identical ion characteristics across the nightside is also not correct, but the injected ion flux is actually not identical because the radial drift at the outer boundary is local time dependent. In addition, even though the Volland-Stern model has been used successfully in modeling the storm-time ring current, more robust electric field models exist that include flow channels and other features for rapid access of the plasma sheet to the inner magnetosphere [e.g., *Chen et al*., 2003; *Khazanov et al*., 2003a; *Jordanova et al*., 2003; *Fok et al*., 2003]. Moreover, *Wygant et al*. [1998] reported inner magnetospheric electric field measurements of up to 6 mV/m during storms, and substorm-associated amplitudes of up to 20 mV/m. The former is probably from partial ring current - driven feedback on the electric field [e.g., *Ridley and Liemohn*, 2002; *Fok et al*., 2003], and the latter is probably from the magnetic field reconfiguration [e.g., *Li et al*., 1998]. The peak electric field of 1.4 mV/m is therefore small compared to these observed peak values. A more sophisticated electric field description that includes rapid access to the inner magnetosphere might yield a different distribution for the hot ions, resulting in a different loss rate. The *Daglis et al*. [2003] conclusion that O^+ can significantly contribute to a two-phase decay of the ring current is, therefore, compatible with the conclusion of this study given the proper electric field description in the inner magnetosphere. For the description chosen for this study, charge exchange is clearly not capable of producing a two-phase decay. Even with these caveats about the electric field model, the Kp = 9 simulation essentially fills the simulation domain with ring current ions, and there was still no sign of a two-phase decay in the total energy content time series. Another caveat to mention is the use of a static dipole magnetic field in these simulations. This is certainly not correct, especially for large storms [e.g., *Tsyganenko et al*., 2003]. Inflation of the field will change the particle trajectories and energies, and therefore alter the loss rates. However, by applying the boundary condition at geosynchronous orbit, it is felt that a dipole field is not prohibitively incorrect. The results presented above, therefore, are qualitatively demonstrative of the relative contributions of flow-out and charge exchange to the decay of the storm-time ring current.

5. CONCLUSIONS

It was shown that a two-phase decay (a sharp transition between fast and slow recovery rates) of the ring current total

energy content is produced when the plasma sheet density is dramatically reduced several hours prior to a sudden reduction in the magnetospheric convection strength. The reverse situation, a convection strength reduction prior to a plasma sheet density decrease, does not produce a two-phase decay signature. A two-phase decay is not visible in the results for simultaneous reduction of these two input parameters. Moderate and strong convection strengths were applied, as well as a typical plasma sheet characteristic energy and an elevated energy (that is, a hot plasma sheet).

The hypothesis that the differential charge exchange rates between hot O^+ (fast) and hot H^+ (slow) can produce a two-phase decay in the ring current. The modeling results presented in this study refute this hypothesis. It was shown that a two-phase decay is formed when the loss lifetime is initially short (less than 10 hours) for some interval at the beginning of the recovery phase, followed by a sudden transition to a much longer loss lifetime (at least double the previous value). Flowout loss was found to be the only process with sufficient intensity and variability to cause a sudden increase in the ring current energy loss lifetime. While charge exchange can yield loss lifetimes below 10 hours (for special configurations of the ring current), is not capable of producing a rapid transition in the loss lifetime. Charge exchange is an exponential attenuation of the distribution, with the shorter loss lifetime particles being removed first, followed by a gradual shift to dominance by the longer lifetime particles. This process cannot cause a sudden jump in the total loss lifetime.

An additional finding is that the O^+ and H^+ charge exchange loss rates are often very similar, and the H^+ loss rate is actually larger than the O^+ loss rate in many of the simulation results. This is because of the short loss lifetime for H^+ at low energies (below 40 keV), which are actually faster than the high-energy O^+ loss lifetimes. Low-energy H^+ ions are therefore rapidly removed from the inner magnetosphere at a rate that is equal to or higher than the rapid loss of high-energy O^+ ions. This balance between the H^+ and O^+ charge exchange loss lifetimes further refutes the hypothesis that differential charge exchange can produce a two-phase decay. Even a delta-function in energy for the incoming plasma sheet particles would most likely not produce significant differential loss, because the L-shell dependence of the charge exchange loss lifetimes would yield a gradual transition in the total loss lifetime for the ring current energy content.

Acknowledgments. The authors would like to thank the sources of funding for this study: NASA grants NAG5-10297 and NAG-10850 and NSF grant ATM-0090165. We would also like to thank the organizing committee of the Chapman Conference on Inner Magnetospheric Modeling for inviting M.W. Liemohn to give a presentation at the meeting.

REFERENCES

Birn, J., M.F. Thomsen, J.E. Borovsky, G.D. Reeves, D.J. McComas, and R.D. Belian, Characteristic plasma properties during dispersionless substorm injections at geosynchronous orbit, *J. Geophys. Res.*, 102, 2309, 1997.

Borovsky, J.E., M.F. Thomsen, and R.C. Elphic, The driving of the plasma sheet by the solar wind, *J. Geophys. Res.*, 103, 17,617, 1998.

Chen, M.W., M. Schulz, L.R. Lyons, and D.J. Gorney, Stormtime transport of ring current and radiation belt ions, *J. Geophys. Res.*, 98, 3835, 1993.

Chen, M.W., L.R. Lyons, and M. Schulz, Simulations of phase space distributions of storm time proton ring current, *J. Geophys. Res.*, 99, 5745, 1994.

Chen, M.W., M. Schulz, G. Lu, and L.R. Lyons, Quasi-steady drift paths in a model magnetosphere with AMIE electric field: Implications for ring current formation, *J. Geophys. Res.*, 108(A5), 1180, doi: 10.1029/2002JA009584, 2003.

Daglis, I.A., The role of magnetosphere-ionosphere coupling in magnetic storm dynamics, in *Magnetic Storms, Geophys. Monogr. Ser*., *vol. 98*, edited by B. T. Tsurutani *et al*., pp. 107-116, AGU, Washington, D. C., 1997.

Daglis, I.A., and J.U. Kozyra, Outstanding issues of ring current dynamics, *J. Atmos. Solar-Terr. Physics*, 64, 253-264, 2002.

Daglis, I.A., R.M. Thorne, W. Baumjohann, S. Orsini, The terrestrial ring current: origin, formation and decay, *Rev. Geophys.*, 37, 407-38, 1999.

Daglis, I.A., J.U. Kozyra, Y. Kamide, D. Vassiliadis, A. S. Sharma, M.W. Liemohn, W.D. Gonzalez, B.T. Tsurutani, and G. Lu, Intense space storms: Critical issues and open disputes, *J. Geophys. Res.*, 108(A5), 1208, doi: 10.1029/2002JA009722, 2003.

Dessler, A.J., and E.N. Parker, Hydromagnetic theory of geomagnetic storms, *J. Geophys. Res.*, 64, 2239, 1959.

Ebihara, Y., and M. Ejiri, Modeling of solar wind control of the ring current buildup: A case study of the magnetic storms in April 1997, *Geophys. Res. Lett.*, 25, 3751, 1998.

Ebihara, Y., and M. Ejiri, Simulation study on fundamental properties of the storm-time ring current, *J. Geophys. Res.*, 105, 15,843, 2000.

Feldstein, Y.I., L.A. Demukhina, U. Mall, and J. Woch, On the two-phase decay of the Dst-variation, *Geophys. Res. Lett.*, 27, 2813, 2000.

Fok, M-C., J.U. Kozyra, A.F. Nagy, C.E. Rasmussen, and G.V. Khazanov, A decay model of equatorial ring current and the associated aeronomical consequences, *J. Geophys. Res.*, 98, 19,381, 1993.

Fok, M.-C., *et al*., Global ENA image simulations, *Space Sci. Rev.*, 109, 77, 2003.

Friedel, R.H.W., H. Korth, M.G. Henderson, M.F. Thomsen, and J.D. Scudder, Plasma sheet access to the inner magnetosphere, *J. Geophys. Res.*, 106, 5845, 2001.

Friedrich, E., G. Rostoker, and M.G. Connors, Influence of the substorm current wedge on the Dst index, *J. Geophys. Res.*, 104, 4567-4575, 1999.

Greenspan, M.E., and D.C. Hamilton, A test of the Dessler-Parker-Sckopke relation during magnetic storms, *J. Geophys. Res.*, 105, 5419, 2000.

Hamilton, D.C., G. Gloeckler, F.M. Ipavich, W. Studemann, B. Wilkey, and G. Kremser, Ring current development during the great geomagnetic storm of February 1986, *J. Geophys. Res.*, 93, 14343-55, 1988.

Jordanova, V.K., L.M. Kistler, J.U. Kozyra, G.V. Khazanov, and A.F. Nagy, Collisional losses of ring current ions, *J. Geophys. Res.*, 101, 111, 1996.

Jordanova, V.K., C.J. Farrugia, L. Janoo, J.M. Quinn, R.B. Torbert, K.W. Ogilvie, R.P. Lepping, J.T. Steinberg, D.J. McComas, and R.D. Belian, October 1995 magnetic cloud and accompanying storm activity: Ring current evolution, *J. Geophys. Res.*, 103, 79, 1998.

Jordanova, V.K., C.J. Farrugia, R.M. Thorne, G.V. Khazanov, G.D. Reeves, and M.F. Thomsen, Modeling ring current proton precipitation by EMIC waves during the May 14-16, 1997, storm, *J. Geophys. Res*, 106, 7, 2001.

Jordanova, V.K., L.M. Kistler, M.F. Thomsen, and C.G. Mouikis, Effects of plasma sheet variability on the fast initial ring current decay, *Geophys. Res. Lett.*, 30(6), 1311, doi: 10.1029/ 2002GL016576, 2003.

Jorgensen, A.M., M.G. Henderson, E.C. Roelof, G.D. Reeves, and H.E. Spence, Charge exchange contribution to the decay of the ring current, measured by energetic neutral atoms (ENAs), *J. Geophys. Res.*, 106, 1931, 2001.

Khazanov, G.V., K.V. Gamayunov, V.K. Jordanova, and E.N. Krivorutsky, A self-consistent model of the interacting ring current ions and electromagnetic ion cyclotron waves, initial results: Waves and precipitating fluxes, *J. Geophys. Res.*, 107(A6), 1085, doi: 10.1029/2001JA000180, 2002.

Khazanov, G.V., M.W. Liemohn, T.S. Newman, M.-C. Fok, and R.W. Spiro, Self-consistent magnetosphere-ionosphere coupling: Theoretical studies, *J. Geophys. Res.*, 108(A3), 1122, doi: 10.1029/2002JA009624, 2003a.

Khazanov, G.V., K.V. Gamayunov, and V.K. Jordanova, Self-consistent model of magnetospheric ring current and electromagnetic ion cyclotron waves: The 2-7 May 1998 storm, *J. Geophys. Res.*, 108(A12), 1419, doi: 10.1029/ 2003JA009856, 2003b.

Khazanov, G.V., M.W. Liemohn, T.S. Newman, M.-C. Fok, and A.J. Ridley, Magnetospheric convection electric field dynamics and stormtime particle energization: Case study of the magnetic storm of 4 May 1998, *Ann Geophys*., 22, 497, 2004a.

Khazanov, G.V., M.W. Liemohn, M.-C. Fok, T.S. Newman, and A.J. Ridley, Stormtime particle energization with high time resolution AMIE potentials, *J. Geophys. Res.*, doi: 10.1029/ 2003JA010186, in press, 2004b.

Korth, H., M.F. Thomsen, J.E. Borovsky, and D.J. McComas, Plasma sheet access to geosynchronous orbit, *J. Geophys. Res.*, 104, 25,047, 1999.

Kozyra, J.U., and M.W. Liemohn, Ring current energy input and decay, *Space Sci. Rev*, 109, 105, 2003.

Kozyra, J.U., M.C. Fok, E.R. Sanchez, D.S. Evans, D.C. Hamilton and A. F. Nagy, The role of precipitation losses in producing the rapid early recovery phase of the great magnetic storm of February 1986, *J. Geophys. Res.*, 103, 6801, 1998.

Kozyra, J.U., M.W. Liemohn, C.R. Clauer, A.J. Ridley, M.F. Thomsen, J.E. Borovsky, J.L. Roeder, and V.K. Jordanova, Two-step Dst development and ring current composition changes during the 4-6 June 1991 magnetic storm, *J. Geophys. Res.*, 107(A8), 1224, doi: 10.1029/ 2001JA000023, 2002.

Lee, L.C., G. Corrick, and S.-I. Akasofu, On the ring current energy injection rate, *Planet. Space Sci.*, 31, 901, 1983.

Li, X., D.N. Baker, M. Temerin, G.D. Reeves, and R.D. Belian, Simulation of dispersionless injections and drift echoes of energetic electrons associated with substorms, *Geophys. Res. Lett.*, *25*, 3763, 1998.

Liemohn, M.W., Yet another caveat to the Dessler-Parker-Sckopke relation, *J. Geophys. Res.*, 108(A6), 1251, doi: 10.1029/ 2003JA009839, 2003.

Liemohn, M.W., and J.U. Kozyra, Lognormal form of the ring current energy content, *J. Atmos. Solar-Terr. Phys.*, 65, 871, 2003.

Liemohn, M.W., J.U. Kozyra, V.K. Jordanova, G.V. Khazanov, M.F. Thomsen, and T.E. Cayton, Analysis of early phase ring current recovery mechanisms during geomagnetic storms, *Geophys. Res. Lett.*, 25, 2845, 1999.

Liemohn, M.W., J.U. Kozyra, M.F. Thomsen, J.L. Roeder, G. Lu, J.E. Borovsky, and T.E. Cayton, Dominant role of the asymmetric ring current in producing the stormtime Dst*, *J. Geophys. Res.*, 106, 10,883, 2001a.

Liemohn, M.W., J.U. Kozyra, C.R. Clauer, and A.J. Ridley, Computational analysis of the near-Earth magnetospheric current system, *J. Geophys. Res.*, 106, 29,531, 2001b.

Liemohn, M.W., A.J. Ridley, D.L. Gallagher, D.M. Ober, and J.U. Kozyra, Dependence of plasmaspheric morphology on the electric field description during the recovery phase of the April 17, 2002 magnetic storm, *J. Geophys. Res.*, 109(A3), A03209, doi: 10.1029/2003JA010304, 2004.

Lyons, L.R., and D.J. Williams, A source for the geomagnetic storm main phase ring current, *J. Geophys. Res.*, 85, 523, 1980.

Maynard, N.C., and A.J. Chen, Isolated cold plasma regions: Observations and their relation to possible production mechanisms, *J. Geophys. Res.*, 80, 1009, 1975.

McComas, D.J., S.J. Bame, B.L. Barraclough, J.R. Donart, R.C. Elphic, J.T. Gosling, M.B. Moldwin, K.R. Moore, and M.F. Thomsen, Magnetospheric plasma analyzer: initial three-spacecraft observations from geosynchronous orbit, *J. Geophys. Res.*, 98, 13,453, 1993.

Mitchell, D.G., K.C. Hsieh, C.C. Curtis, D.C. Hamilton, H.D. Voss, E.C. Roelof, and P. C:son Brandt, Imaging two geomagnetic storms in energetic neutral atoms, *Geophys. Res. Lett.*, 28, 1151, 2001.

Ober, D.M., J.L. Horwitz, and D.L. Gallagher, Formation of density troughs embedded in the outer plasmasphere by subauroral ion drift events, *J. Geophys. Res.,* 102, 14,595, 1997.

O'Brien, T.P., R.L. McPherron, and M. W. Liemohn, Continued convection and the initial recovery of Dst, *Geophys. Res. Lett.*, 29(23), 2143, doi: 10.1029/2002GL015556, 2002.

Ohtani, S., M. Nosé, G. Rostoker, H. Singer, A.T.Y. Lui, and M. Nakamura, Storm-substorm relationship: Contribution of the tail current to *Dst*, *J. Geophys. Res.*, 106, 21,199, 2001.

Pollock, C.J., *et al*., First medium energy neutral atom (MENA) images of Earth's magnetosphere during substorm and storm-time, *Geophys. Res. Lett.*, 28, 1147, 2001.

Rairden, R.L., L.A. Frank, and J.D. Craven, Geocoronal imaging with Dynamics Explorer, *J. Geophys. Res.*, 91, 13,613, 1986.

Reeves, G.D., and H.E. Spence, Charge exchange contribution to the decay of the ring current measured by energetic neutral atoms (ENAs), *J. Geophys. Res.*, 106, 1931-1937, 2001.

Sckopke, N., A general relation between the energy of trapped particles and the disturbance field near the Earth, *J. Geophys. Res.*, 71, 3125, 1966.

Søraas, F., K. Aarsnes, K. Oksavik, and D.S. Evans, Ring current intensity estimated from low altitude proton observations, *J. Geophys. Res.*, 107, 1149, doi: 10.1029/2001JA000123, 2002.

Søraas, F., K. Oksavik, K. Aarsnes, D.S. Evans, and M.S. Greer, Storm time equatorial belt—an "image" of RC behavior, *Geophys. Res. Lett.*, 30(2), 1052, doi: 10.1029/ 2002GL015636, 2003.

Stern, D.P., The motion of a proton in the equatorial magnetosphere, *J. Geophys. Res.*, 80, 595, 1975.

Takahashi, S., T. Iyemori, and M. Takeda, A simulation of the storm-time ring current, *Planet. Space Sci.*, 38, 1133-1141, 1990.

Takahashi, S., M. Takeda, and Y. Yamada, Simulation of storm-time partial ring current system and the dawn-dusk asymmetry of geomagnetic variation, *Planet. Space Sci.*, 39, 821, 1991.

Tinsley, B.A., and S.-I. Akasofu, A note on the lifetime of the ring current particles, *Planet. Space Sci.*, 30, 733, 1982.

Tsyganenko, N.A., H.J. Singer, and J.C. Kasper, Storm-time distortion of the inner magnetosphere: How severe can it get?, *J. Geophys. Res.*, 108(A5), 1209, doi: 10.1029/ 2002JA009808, 2003.

Turner, N.E., D.N. Baker, T.I. Pulkkinen, and R.L. McPherron, Evaluation of the tail current contribution to Dst, *J. Geophys. Res.*, 105, 5431, 2000.

Volland, H. A semiempirical model of large-scale magnetospheric electric fields, *J. Geophys. Res.*, 78, 171, 1973.

Walt, M., and H.D. Voss, Losses of ring current ions by strong pitch angle scattering, *Geophys. Res.*, *Lett.*, 28, 3839, 2001.

Wygant, J., D. Rowland, H.J. Singer, M. Temerin, F. Mozer, and M.K. Hudson, Experimental evidence on the role of the large spatial scale electric field in creating the ring current, *J. Geophys. Res.*, 103, 29,527, 1998.

J.U. Kozyra and M.W. Liemohn, Atmospheric, Oceanic, and Space Sciences Department, University of Michigan, 2455 Hayward St., Ann Arbor, MI 48109-2143 (liemohn@umich.edu, jukozyra@umich.edu).

Query

Q1 Please check <E> this is needed here.